

Research Paper

GBD-DART-I : Pulsars and transient source observation between 130 MHz and 350 MHz at Gauribidanur

Arul Pandian B^{1,2}, Joydeep Bagchi¹, Prabu Thiagaraj², K.B.Raghavendra Rao², Vinutha Chandrashekhar², R Abhishek², Arasi Sathyamurthy², Sandhya², Sahana Bhatramakki², Kasturi S², Shiv Sethi²

¹Department of Physics and Electronics, CHRIST (Deemed to be University), Bangalore, India., ²Raman Research Institute, Bangalore 560080, India.

Abstract

Gauribidanur Diamond Array Radio Telescope (GBD-DART) is a new small LPDA antenna array consisting of 64 short dipoles and associated receivers that has been custom developed and deployed at the Gauribidanur observatory (13.604 N, 77.427 E) to study bright Pulsars and Solar transients in the frequency range of 130-350 MHz. The LPDAs are arranged in a checkerboard layout, with opposite pairs combined to enable dual-polarised operation. A diamond-shaped (tilted square) array configuration was chosen to achieve high sidelobe suppression in the East-West and North-South directions. The tile measures 5.9 meters by 5.9 meters, with diagonals along both the North-South and East-West directions, each measuring about 8.4 meters. The LPDA array with one diamond-shaped tile has been fully commissioned and is operating in transit-observing mode, successfully detecting strong pulsars and solar flares over the last seven months. The present digital backend restricts the instantaneous bandwidth for observations to 16 MHz. The array operations are streamlined to facilitate remote operations. Apart from investigating Pulsar and Solar phenomena at low radio frequencies in selected sources, this work aims to provide a training platform for radio astronomy through simple-to-construct, low-cost radio telescopes. In this paper, we present details of the array, including antenna and array response studies, brief descriptions of front-end and backend instrumentation, and illustrative results from observations of both pulsars and solar flares. It will also provide brief details of future upgrade plans, particularly for the tiles and digital backend, to facilitate the observation of additional sources.

Keywords: Aperture array, dipoles, LPDA, dual polarized antenna, high gain, antenna gain, side-lobe rejection, pulsars, solar flares,

(Received xx xx xxxx; revised xx xx xxxx; accepted xx xx xxxx)

1. Introduction

Our understanding of the Universe has significantly expanded due to radio astronomy, which has changed our perspectives. There are several important benefits to low-frequency radio observation. Numerous celestial objects are coherent continuum sources, such as pulsars, which emit synchrotron radio with a steep spectrum that intensifies substantially at low frequencies. The desire to investigate the distant Universe using the highly redshifted 21-cm line of neutral hydrogen (HI) at the epoch of reionisation (Morales MF. *et al.* 2004; Benson AJ. *et al.* 2006), cosmic microwave background radiation (Penzias AA. *et al.* 1965), the study of the dark halo with the galactic rotation curve (Sofue Yoshiaki 2020), The Sun (Ramesh R. *et al.* 1998), neutron stars and pulsars (Hewish A. *et al.* 1969), an understanding of the interstellar medium probogation effect with fast radio bursts (Petroff E. *et al.* 2019), the frequency-dependent study by plasma dispersion (Cordes JM. *et al.* 2016), magnetic field strength with faraday rotation (Lyne AG. *et al.* 1989). Low-frequency radio observations of pulsar emissions (Singha J. *et al.* 2021) and timing measurements (Backer DC. *et al.* 1986; Tarafdar P. *et al.* 2022) are crucial

for comprehending and characterising the effects of the interstellar medium. These observations help investigate phenomena such as chromatic dispersion, scintillation, and pulsar emission spectra. This information helps determine the timing of pulsar signals, thereby improving advanced investigations of gravitational wave detection. (Srivastava A. *et al.* 2023; Bhat NDR. *et al.* 2018).

Several large and modern aperture array radio telescopes, such as the Low-Frequency Array (LOFAR) (van HMP. *et al.* 2013), the Long Wavelength Array (LWA) (Ellingson SW. *et al.* 2009), the Murchison Widefield Array (MWA) (Tingay SJ 2013), the Canadian Hydrogen Intensity Mapping Experiment (CHIME) (Amiri M. *et al.* 2018), the Hydrogen Epoch of Reionisation Array (HERA) (DeBoer DR. *et al.* 2017), and the upcoming Square Kilometre Array (SKA) (Dewdney PE. *et al.* 2016) designed to probe the low/mid radio frequency universe. The radio observatory at Gauribidanur facilitated pulsar observations at 34.5 MHz using a fat-dipole array (Sastry ChV. 1989; Deshpande AA. *et al.* 1992; Maan Y. 2015), and between 50 and 80 MHz using an LPDA array (Bane KS. *et al.* 2022).

The new LPDA antenna array presented in this paper is designed to observe pulsars and solar transients at 130-350 MHz from the Gauribidanur Observatory. Additionally, we aimed to provide a cost-effective, simple radio telescope design for educational purposes, enabling a larger number of university students to engage in hands-on training in radio astronomy, particularly in pulsar and solar observations. The use of an LPDA-based aperture

Author for correspondence: Arul Pandian B, Email: arulpandian022@gmail.com
Cite this article: Author1 C and Author2 C, an open-source python tool for simulations of source recovery and completeness in galaxy surveys. *Publications of the Astronomical Society of Australia* **00**, 1–12. <https://doi.org/10.1017/pasa.xxxx.xx>

array in the design achieved cost-effectiveness and broadband frequency coverage (Isbell D. *et al.* 2003). Finding radio-frequency interference (RFI)-free zones and suitable array configurations to maximise the array gain required significant investigations (Arul PB. *et al.* 2022), (Arul Pandian B 2025). The functionalities of the antenna, signal conditioning, and signal transport components were first verified in a two-element interferometer setup (Likhit AASR. *et al.* 2025). Subsequently, a 64-dipole tile was commissioned at the observatory site. The 64 LPDAs of the array are phased to observe transiting sources nominally for about an hour at the zenith. The current instantaneous observing bandwidth is 16 MHz per polarisation, with the restriction imposed by the data recorder. The array observations can be remotely scheduled and monitored. Work is also in progress to implement a second tile to enhance observations.

This paper outlines how we addressed the design challenges of implementing a radio array, its end-to-end functionality, and the results of observations of radio pulsars and solar transients. Section 2 discusses the project's motivation, design considerations, and choices made during the process. Section 3 examines the antenna responses investigated for different LPDA configurations, ranging from a single dipole to a diamond-shaped array. Section 4 introduces the signal conditioning, transport, data capture, and analysis pipeline to validate the end-to-end system in the field. Section 5 presents the results of field testing the system. Finally, section 6 provides a summary of the work, highlighting future directions and conclusions.

2. Array Design considerations

A significant constraint on the array design arises from pulsar observations; pulsar signals are extremely weak compared to those from the Sun, and they are point-like sources in the sky. Hence, one primary consideration for the array is to achieve good sensitivity at 150-200 MHz, as at these frequencies the pulsars are typically bright and tend to show emission turning points. A second consideration arises because pulsar signals originate from unresolvable tiny angular regions in the sky; the array's ability to measure broadband signals from pulsars over a narrow area of the sky without grating or side-lobe contamination is crucial.

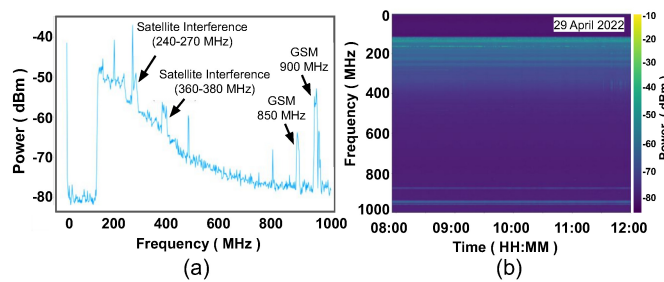


Figure 1. Typical (a) spectrum and (b) spectrogram observed in the RFI measurements at the Gauribidanur observatory from 2022.

We studied the site's RFI conditions over several days, using a custom-built receiver chain and a commercial spectrum analyser (Arul Pandian B 2025). An illustration of a typical spectrum obtained with the most numerous interferences is shown in Figures 1a and 1b. Strong RFI was observed between 80 MHz and 129 MHz, and moderate levels of RFI were detected between 250

MHz and 270 MHz, as illustrated in the figures. Typically, strong low-frequency (below 130 MHz) RFI saturated the measurement system's front-end amplifiers. Hence, we used a high-pass filter to eliminate low-frequency RFI bands (below 129 MHz) for the RFI study, and also set the array's lowest frequency to 130 MHz. The highest frequency for the antenna array was limited to 350 MHz due to the interference seen beyond this frequency.

3. LPDAs in a Diamond Configuration

We designed the aperture array using a set of 64 short LPDAs, which was previously custom-designed in our laboratory (Arul Pandian B 2025). The LPDA shown in Figure 2a is an optimised version of it, mainly to operate within the 130-350 MHz frequency range, and its performance verified through beam pattern simulations shown in Figures 2b and 2c, and through the S11 simulations and verifications in the field as shown in Figure 3. The LPDA consisted of 11 dipole elements, each constructed from a 9 mm-diameter aluminium alloy round tube with a 1 mm wall thickness. The booms of the LPDA are fabricated from a 12 mm aluminium alloy square tube with a 1 mm wall thickness. The dipoles are connected to the boom by welding.

To get the orthogonal X and Y polarisations, we have examined arranging *two-pairs of LPDAs* in an off-axis arrangement (Shankar NU. *et al.* 2009; Maan Y. *et al.* 2013) as shown in Figure 2d. In this configuration, the voltages of opposite LPDAs are combined to form the two polarisation feeds with their electrical centre at the baseline's centre. Simulations indicate achieving a symmetric response across the broadband with a nominal 60° field of view and 11 dBi gain as shown in Figures 2e and 2f.

Our investigation into arrays identified a novel diamond (a 45° rotated square) configuration (kraus JD. *et al.* 1967, 2011). A simple model of it was first studied using both *Python* based and CST® designs. We enhanced the configuration with two additional features. First, we arranged the dual-polarised LPDA pairs in a checkerboard layout (Kawano T. *et al.* 2016, 2017; Hotan AW. *et al.* 2021) within the diamond shape. Next, we positioned the LPDA pairs at an inclined angle of 23° from the zenith (67° from ground) with the tilt being towards each other within the pair as is shown in 2d. The resulting array exhibited near-flat gain across the band and significant sidelobe suppression in the East-West and North-South directions, both highly desirable. The far-field orthographic responses (obtained using CST) of the array with one, two, eight and 32 LPDAs at 150, 250 and 350 MHz are given in 5.

4. Tile Signal Flow

4.1. Overview

The array is located approximately 250 meters away from the observatory's receiver room. A comprehensive radio-frequency signal conditioning electronics: the analog front-end receiver, a fiber transmission/reception module: RFoF module, were specially developed; and an existing backend digital receiver: PDR was employed for data recording; and also a new set of software utilities for real-time data capture, data processing and archival was developed and executed as pipelines across *Intel-i7* and *AMD-Ryzen-9* desktops to process and store the acquired data (Arul Pandian B 2025). This section provides an overview of the array signal conditioning and data processing. A detailed discussion of it is presented in (Arul PB. *et al.* 2026).

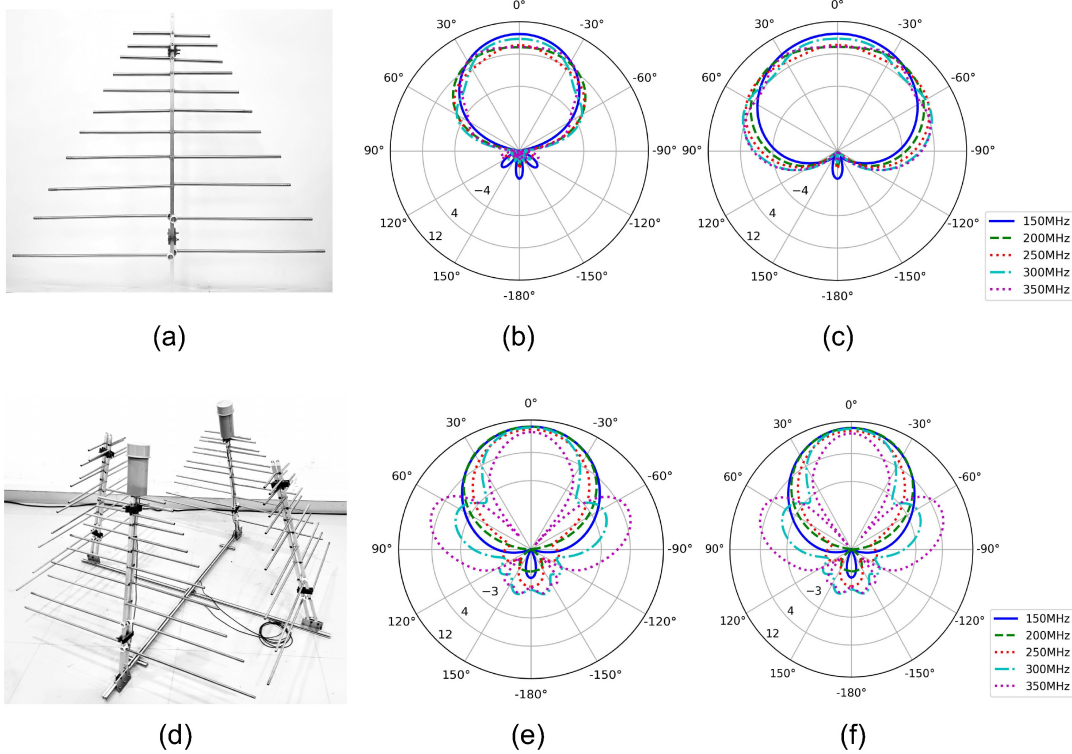


Figure 2. (a) Single LPDA Antenna. The second boom with complement dipoles is joined along the side to form the 11-element LPDA. The responses obtained at 150, 200, 250, 300 and 350 MHz are overlaid for E-plane in (b) and H-plane in (c). (d) Pyramid antenna element (e) Pyramid antenna element E-plane gain (f) Pyramid antenna element H-plane gain . The simulations carried out using the CST® software package

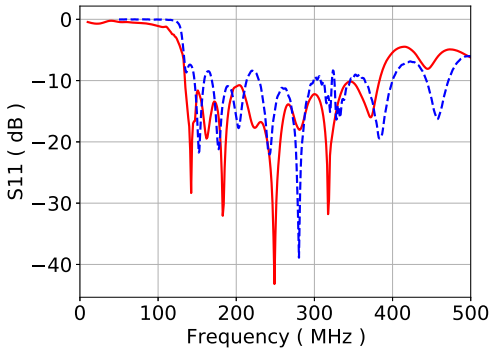
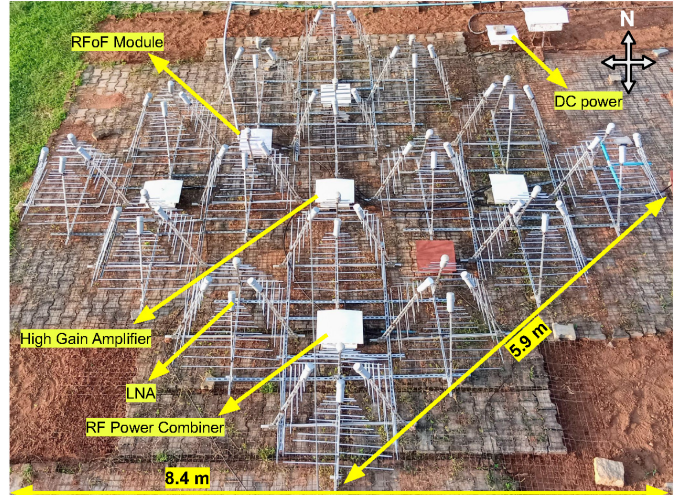


Figure 3. Simulated S11 (blue dashed line) of the LPDA from CST software is compared with measured S11 (solid red line) by N9916B microwave analyser.



4.2. Signal Conditioning and Transport

As outlined in Figure 6, the tile analog signal chain begins with low-noise amplifiers (LNAs) fitted at the boom feed points of the 64 LPDAs (corresponding to 32 X and 32 Y polarisation) through a BALUN arrangement. The LNAs have a 20 dB gain and a bias-tee arrangement to obtain the DC power. The amplified signal leaves the LNAs via a 3-meter-long RG-174 RF cable. The voltage signals from the X- and Y-polarisation LPDAs are combined independently using equal-length wires to produce the tile's phased-array voltage outputs for the two polarisations by combining them in two stages: eight 8-way combiners in the first stage

Figure 4. Diamond antenna array deployment in the field. White boxes seen house first stage analog electronic components. A metal mesh with gap of 1/16 th wavelength of the highest operating frequency isolates the array from ground.

and two 4-way combiners in the second. The first-stage combiners incorporate a bias-tee network for distributing the DC supply to the LNAs.

The tile's voltage outputs are further amplified by a high-gain amplifier stage in a tubular receiver (TubRx) module. It consists of multiple-stage amplifiers and filters arranged in the following

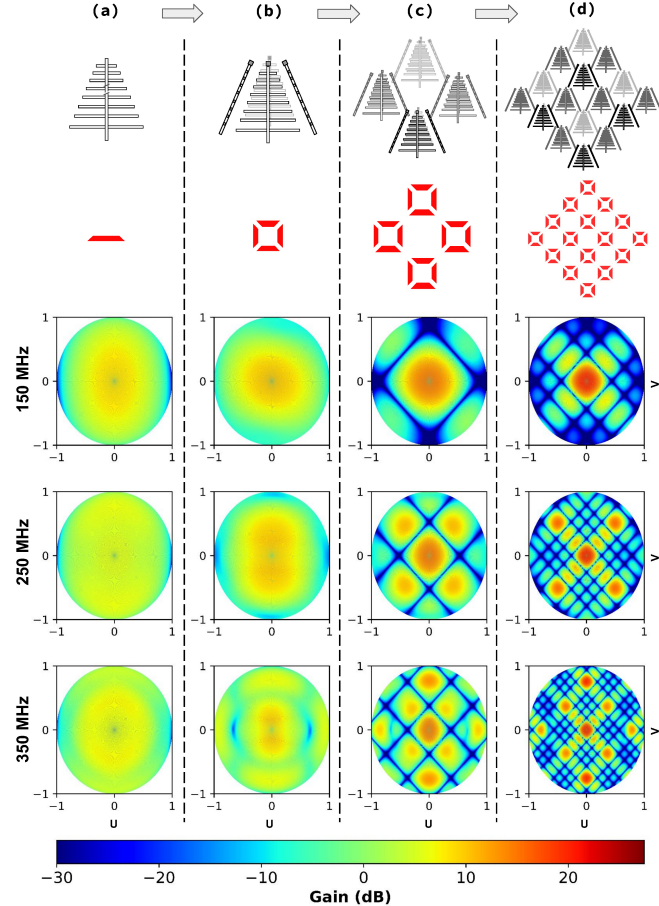


Figure 5. Far-field orthographic responses of the diamond array with only single, two, eight and 32 LPDAs at 150, 250 and 350 MHz

sequence: a first stage amplifier, a high-pass filter allowing signals above 130 MHz, a second amplifier, a Low-pass filter to stop signals above 350 MHz, and a third amplifier. The TubRx has a noise figure of 1.2 dB and a gain of 52 dB across the 220 MHz-wide band from 130 to 350 MHz. The amplified RF signals from the TubRx are routed to an RF over Fiber (RFoF) transmitter (RFoF-Tx) module via a short RF cable.

The RFoF-Tx module is fitted with a pre-amplifier to bias the laser diode, and it has a dynamic range of 40 dB with an operating midpoint at -40 dBm. The RFoF-Tx converts the RF signal amplitudes to a 1310 nm laser output. The transmission is by the intensity modulation of the laser output. A commercial 12-core, 250-meter-long single-mode fiber cable carries the laser signals to the observatory receiver room.

The electronics located in the observatory room, as shown on the right side of figure 6, receive the optical signals from the field in an RF over fiber receiver (RFoF-Rx) module that converts the laser signal to analog RF signal. A one-meter long semi-flex cable with a shield attenuation of about 40 dB was used to carry the RF signal from the RFoF-Rx to a portable dual receiver (PDR) for subsequent band selection, digitisation, and recording of the two polarisation signals.

4.3. Data-Processing

The portable dual receiver (PDR) is a dual-channel, 16-MHz-wideband heterodyne receiver and digitiser. The PDR can select any 16 MHz bands within the 220 MHz wide band received from the array. The PDR has dual 8-bit digitisers sampling at 33 MSPs. The sampled data from the two digitisers are timestamped, packed into a UDP packet, and sent over the Ethernet ports to a data recording computer. An onboard Virtex-5 FPGA is used in the PDR for time stamping and packetisation.

The UDP packets are first captured in the data recording computer (PC1) in a RAM-based circular buffer by using the GULP utilities (Corey Satten. 2008). The captured data fills the circular buffer at a nominal rate of 66 Mbps. The GULP writes the data in a PCAP format. A dedicated process in the PC-1 takes a copy of the data from the circular buffer, computes all correlation products via an FFT, performs a temporal average, and archives the data with timestamps. This archive is written in an HDF5 format. The archived data is used to verify the system's health and monitor the radio spectrum. For pulsar observations, the high time resolution voltage data from the ring-buffers are moved through a transient buffer to the hard disks for post processing (Arul PB. *et al.* 2026).

5. Results from the Array

We present four different results from commissioning the array to illustrate it's end-to-end operation:

- Satellite and Sun transit observations
- Drift observation over days
- Solar transient detection
- Pulsar signal detection

5.1. Satellite and Sun transit observations

We observed ORBCOMM satellite signals at 137 MHz by configuring the PDR mixer's local oscillator to select the lowest 16 MHz frequency band. The data were collected for a full day to cover multiple satellite passes. Figure 7a illustrates a cross-section of the beam, traced during the satellite transit. A drift observation of the Sun was also made, using a band centred around 200 MHz, and the results are presented in figure 7b. In both observations, a subgroup configuration with 8 LPDAs, as shown in Figure 5, was used, and the observed side-lobe levels of around -20 dB, agree with the simulations.

5.2. Drift Observation over days

Drift mode observations in a sub-array configuration of Figure 5c for a 16 MHz band around 200 MHz were made on multiple days to study the receiver performance over the day and against the sky temperature variations. The measured power throughout the day was compared with that expected for the sub-array's beam at the sky positions. On the 408 MHz skymap (Remazeilles M. *et al.* 2015), a 90° declination range strip centred at +13.6° N (instrument zenith) was convolved with the subgroup beam of Figure 5c (Arul Pandian B 2025). The estimate thus-obtained is plotted as a black dot-dashed line in the upper subplot of Figure 8. The different days measurements were normalised to the galactic plane's peak power at 18:30 hours and overlaid in various colours. The estimate matches the power observed by the array, with minor deviations. The Sun (≈ 96000 Jy source) positions shown as the

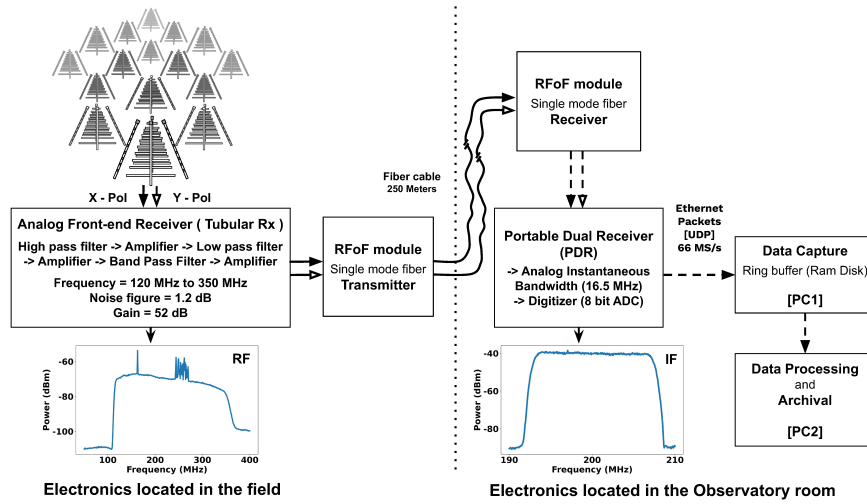


Figure 6. Array signal chain consists of 64 LPDAs in a dual polarised configuration with LNAs, voltage combiner network, high gain amplifiers with 130 to 350 MHz band-pass filters, RF to optical converters, 300 m long 1310 nm single mode optical fibers, optical to RF converters, amplifiers, 16 MHz portable analog/digital receiver, and data recording/processing/archival computers.

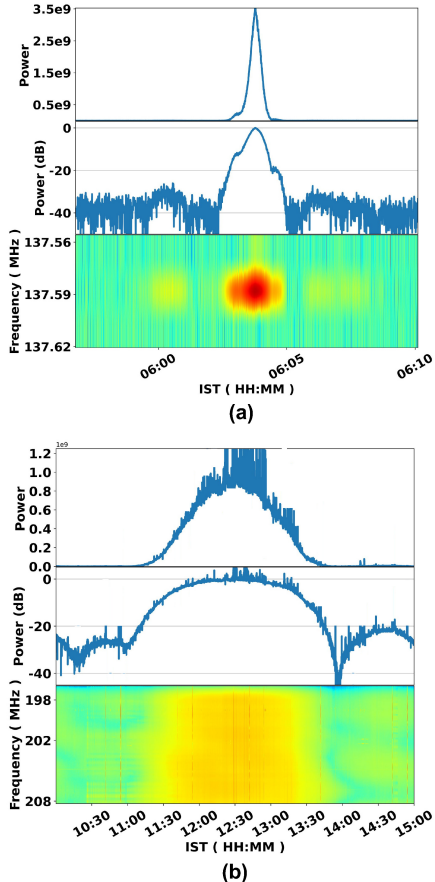


Figure 7. The array's sub-group beam response study using a sub-group of eight LPDAs. (a) Transit observation of ORBCOMM satellite pass at 137 MHz. (b) Transit observation of the Sun at 200 MHz. See also figure 8 for a multiple day transit observation.

yellow dots (P1 and P2) in figure, drifts to the right during the observed epochs between 22 March 2025 and 14 April 2025.

We have also investigated the array's responses to a few radio sources: Cygnus-A (8100Jy), Taurus-A (1420Jy), Virgo-A (970Jy) at 178 MHz (kraus JD. *et al.* 1967) and infer the array subgroup (Eight LPDAs) sensitivity to be around ≈ 250 Jy for 0.5 second integration with ≈ 2 MHz bandwidth.

5.3. Solar Flare Detection

During the system commissioning period, continuous drift mode observations were conducted for system monitoring and pipeline development. Receivers recorded array data for a few hours each day during the solar transit for several months. In figure 9a, we present an intense type III Solar event (solar flare) of 27 July 2024 from the archival data captured by the array. The data have a temporal resolution of 0.5 seconds and a spectral resolution of 64 kHz. The observation was carried out at 200 MHz with a 16.5 MHz bandwidth from 9:00 AM to 3:00 PM local time. The solar event intensity across the observed band is shown on the top plot, and the dynamic spectrum obtained during the event is displayed in the bottom-left subplot. The spectrum observed during the event is given in the bottom-right plot. The observation data corresponding to the results presented are available on GitHub (Arul Pandian B 2025). We find that our detection time and event morphologies significantly matched the same event recorded by the e-CALLISTO Solar Radio Spectrograph at the Udaipur Solar Observatory (Upadhyay K. *et al.* 2019).

The antenna power deflection during the solar event is shown in the top subplot. The right-hand subplot shows channel power as a function of frequency. The central subplot shows the dynamic spectrum over time, with frequency along the Y-axis. This spectrogram shows dynamic changes in power across channels over time, with increasing intensity from blue to red.

5.4. Pulsar Signal Detection

A primary focus of this array design was to observe a set of bright pulsars. Hence, we continually developed strategies and tools for observations and data processing (Arul PB. *et al.* 2026). On 14th April 2025, the array had its first light, detecting pulsar B1919+21

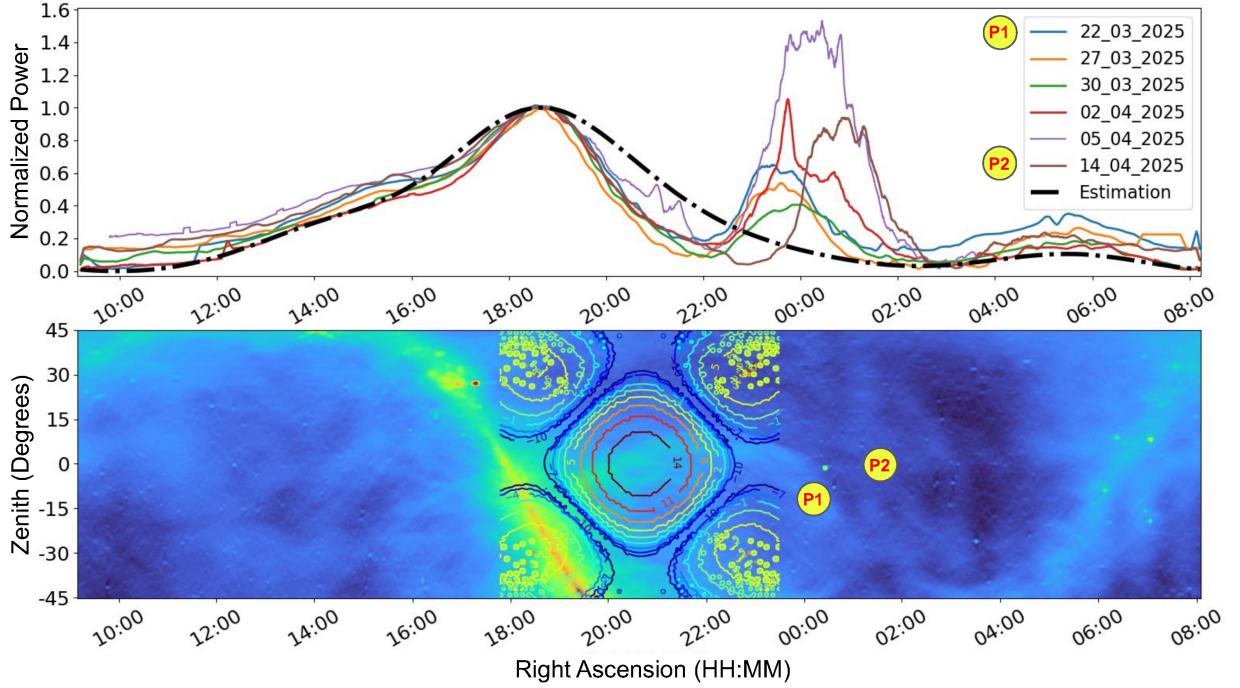


Figure 8. The upper plot shows an overlay of results from six days' drift mode observation by the array subgroup Figure 5c. High intensities correspond to the Galactic plane, which is visible at RA 18:30, and is obscured by the Sun between 23:00 and 02:00 Hours. The plots correspond to observations made over three weeks. The lower subplot shows the radio sky visible to the array's subgroup in the (Remazeilles M. *et al.* 2015) 408 MHz sky map. An orthographic beam pattern of the array subgroup at 200 MHz is overlaid on the sky map. This orthographic pattern was convolved with the sky map to estimate the expected total power deflections from the subgroups (shown as a black dot-dashed line in the upper plot). The total power observed was normalised to the peak power in the galactic plane at 18:30 hours. The positions of the Sun at the beginning of this set of observations on 22 March 2025 and at the end of the observation on 14 April 2025 are marked as P1 and P2, respectively, on the map.

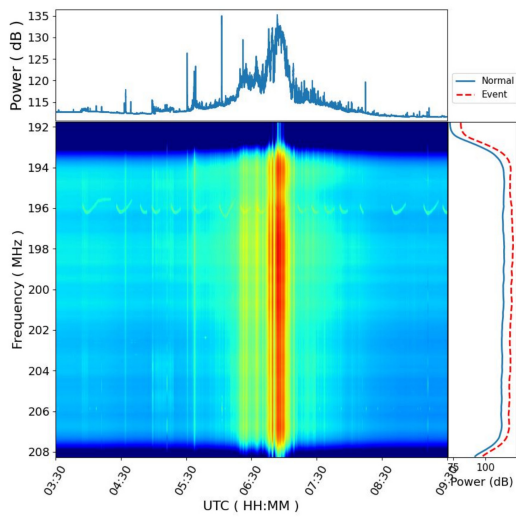


Figure 9. An intense solar event recorded on 27 July 2024.

with an SNR of 7, using only 16 LPDAs across two X-polarisation subgroups. Subsequently, we have brought up the whole array with 64 LPDAs as outlined in the paper with dual (X and Y) polarisation and successfully detected four other bright pulsars that transit across the array's nominal half-power beam between declination of $+6^\circ$ and $+22^\circ$ (Figure 11). A dedicated pulsar data processing pipeline was built with the standard software packages such

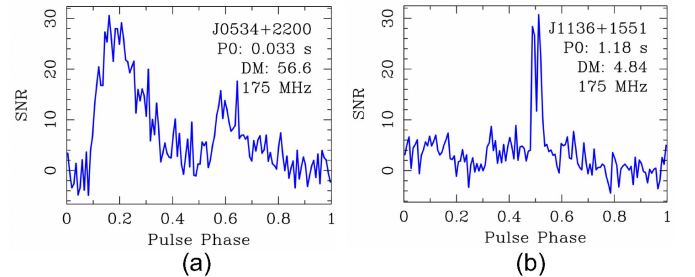


Figure 10. Pulsars detected at 175 MHz with 1800 seconds integration. (a) J0534+2200 (MJD 60945) (b) J1136+1551 (MJD 60939)

as DSPSR (van Straten. W. & Bailes. M. 2011) and PSRCHIVE (Hotan A. W. *et al.* 2004). The continuous raw ADC data was recorded with the PDR system (Figure 6). The data were reduced to a time resolution of $128\ \mu\text{s}$ and a spectral resolution of 64 kHz, with all stokes products in PSRFITS format (Hotan A. W. *et al.* 2004). We present in Figure 10, a folded total intensity pulse profile for two pulsars, J0534+2200 (CRAB pulsar) and J1136+1551. They were observed with the full array in the dual-polarised LPDA arrangement described in the paper, over a 16 MHz band centred at 175 MHz and an integration time of 1800 seconds. The intensities from the two polarisations were added during post-processing. These two pulsars represent the extremes of dispersion measures and periods in our sample of five currently detected pulsars: J0953+0755, J0837+0610, and J1921+2153, which are

routinely detected by the array. The relevant findings from these additional pulsars are presented in (Arul PB. *et al.* 2026).

6. Future Scopes

The array's system noise temperature of ≈ 250 Jy for 0.5-second integration with ≈ 2 MHz bandwidth was estimated by observing Virgo-A. The signal strength of pulsars in our frequencies of interest typically ranges from a few milli-Jansky to a few thousand Jansky. There are 16 dual-polarised elements in the array, each with a typical gain of 10.5 dBi throughout the band, resulting in an effective aperture area of 30 m^2 , an array gain of 22 dBi and a system equivalent flux density (SEFD) of 25 kJy. Thus, if we consider a 16 MHz band observation over an hour with a nominal HPBW of 15 degrees at 200 MHz, the system will be sensitive enough to detect sources with a flux density of 50 mJy.

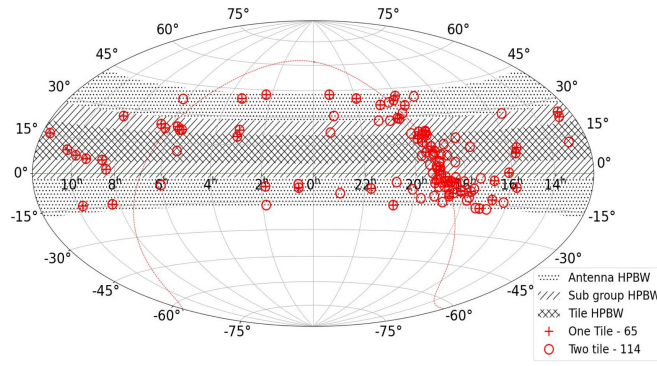


Figure 11. The sky visible to a GBD-DART tile, and detectable pulsars. The hatched region depicts the HPBW of the primary X- and Y-polarisation LPDAs. A narrower inner shaded sky area is visible for the 16 LPDA subgroup beams. The '+' symbols on the map indicate the locations of the 65 pulsars detectable with a reasonable SNR (10) in an hour of observation in a 16 MHz band around 200 MHz. The 'O' symbols indicate the locations of 114 pulsars that can be detected by doubling the collecting area (two tiles).

Figure 11 displays the regions of sky and pulsars in those regions that have flux above 50 mJy at 200 MHz, and hence are detectable for different configurations of the array. The sky areas shown by the three patches in the figure correspond to the skies that become visible in three different beamforming modes of observation. The sky region indicated by the central patch corresponds to the sky observable by a tile with its zenith beam (current mode), as determined by combining all LPDAs. The adjoining patch of the sky becomes visible to the array in groups of 8 dipoles, phased separately and combined. With this mode, additional pulsars can be observed. The outside patch area of the Sky becomes observable if the beams are formed at the individual dipole element level of a tile. The number of pulsars shown in the legend of figure 11b is based on the theoretical estimation (Lorimer DR. and Kramer M. 2015), considering the sensitivity limits of a single tile.

The array's response towards three different pointing directions at two different frequencies was simulated in CST, and the results are shown in Figure 12. To obtain the arrays' steered-beam responses, we first created the antenna array element positions in CST, exported them to a custom-developed computer code, and estimated the phase required for each primary element to steer the beam. Then, we applied these phases to the excitation ports in the CST simulation and obtained orthographic responses for

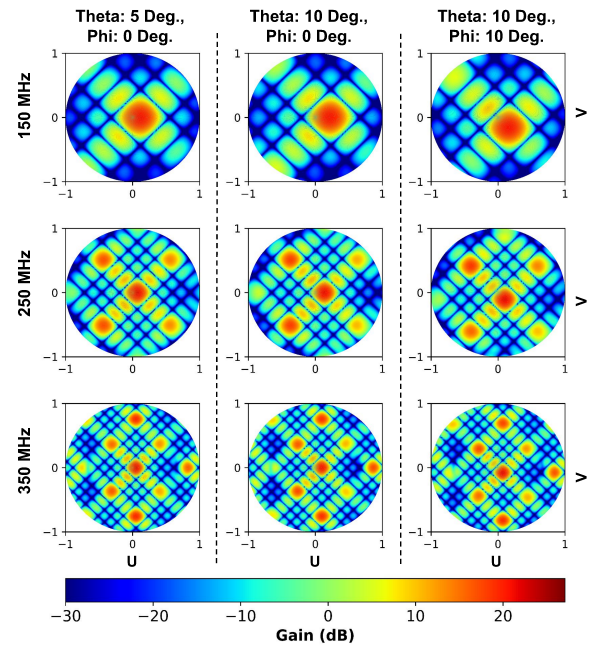


Figure 12. Illustration of beam positions across the band with phasing. A time-delay-based beam-forming method enables wider tracking and pointing.

each pointing set. Figure 12 presents the beam formation at the two extreme frequencies towards three directions in the sky.

We would also investigate forming multiple simultaneous beams for transient watch/search applications in such a case. An FFT-based beamforming option can be investigated for this array (Arul Pandian B 2025). Multiple beams are beneficial for transient searches, such as investigations into Fast Radio Bursts (FRBs).

The sensitivity can also be improved by increasing the number of tiles and enhancing the associated signal conditioning and processing.

Our current digital back-ends record only a 16 MHz band, and we would also consider recording and processing larger bands up to 200 MHz. These efforts would involve upgrading the digital receivers to higher-capability FPGA-based receivers, such as those recently developed in the lab (Girish B. S. *et al.* 2023).

7. Summary and Conclusion

We have designed and implemented an array of log-periodic antennas (LPDA) in a diamond configuration, (measuring 5.9 meters by 5.9 meters, with its diagonals aligned along both the North-South and East-West directions) at the Gauribidanur observatory (GBD-DART). It is a small array with 64 LPDAs arranged in a checkerboard layout, forming orthogonal polarisation with dual-tilted LPDAs. This array is primarily employed to study bright Pulsars and Solar transients in the frequency range of 130-350 MHz. The diamond-shaped (tilted-square) array configuration helped suppress sidelobes. It enabled pulsar observations, often without being affected by strong signals from the Sun or other bright radio objects in the Sky, or by any low-level RFI from the horizon. All associated electronics for the array have been custom-developed and commissioned on-site. The antennas, RF front-end, fiber transmission system, back-end RF and digital systems, as

well as the data-gathering and processing pipelines, are all developed in-house, and their salient features are outlined in this paper and a detailed discussions about the specialised signal processing pipeline developed to perform astronomical data analysis, particularly for pulsar data processing in (Arul PB. *et al.* 2026). The array beam formations were studied through simulations and verified by observing satellite signals and strong celestial sources. The array also continuously collects 1 s time-resolution spectral data in a 24x7 manner, and from this archival data we detected a strong radio flare from the Sun, with the event time and morphologies verified against established observatory results. The array's ability to detect weak radio sources is demonstrated through the successful observation of five bright pulsars of varying periods, flux densities, and dispersion measures. These pulsar parameters, including profile and dispersion measure, detected by the array significantly match the standard catalogues, confirming that our frequency and timing standards are well understood and meeting the standards for such time-domain astronomy. Currently, we can observe pulsars with flux densities above 700 mJy and that transit our nominal zenith beam between +8° and +21° declination for about an hour. However, we discussed schemes to enhance the array sensitivity and detect about 10 times weaker sources. One of the primary focuses of this array building effort is to illustrate how a small radio telescope can be built to observe radio transients such as pulsars, and to leverage duplication of such designs to enhance the number of student participants both in the instrumentation and in understanding the radio pulsar observations, data analysis, and develop interest in pulsar astrophysics. This new small pulsar array is open for student training, offering hands-on experience in observations, data analysis, and signal processing for astrophysics (Adithya P. 2025), (Mahek P. 2025).

Disclosures

The authors declare there are no financial interests, commercial affiliations, or other potential conflicts of interest that have influenced the objectivity of this research or the writing of this paper.

7.1. Conflicts of Interest

None.

Code, Data, and Materials Availability

The data presented in this article are publicly available in https://github.com/Arul16psp05/supplementary_materials.git at <https://doi.org/10.5281/zenodo.15709357>

Acknowledgments

We acknowledge the multiple technical consultations with R. Somashekar. We also value Keerthipriya Sathish for guiding the development of the RF over fiber transmission links. We acknowledge the involvement of our colleagues at the Gauribidanur Observatory team for their support during the commissioning of the LPDA array, particularly Srinath and Janardhanan, and for their contributions to making all of the 64 LPDAs and in making the RF module enclosures at the observatory workshop and Ibrahim for the access to the RRI workshop. Additionally, we thank the undergraduate interns at Gauribidanur AES National

College for their help in transporting and mounting the array of elements from the Bangalore lab to the observatory. We are also grateful to our EEG colleagues for their various forms of support and valuable conversations that aided this work. We thank the Raman Research Institute for supporting this development work. We also thank the Christ University for recognizing the research aspect of this effort. Also, we acknowledge the use of the RRI library, which provided access to the Grammarly (Fitria Tira Nur. 2021) tool and the publicly available QuillBot (Fitria Tira Nur. 2021) to correct grammar in the manuscript.

References

Morales, Miguel F and Hewitt, Jacqueline., (2004). 'Toward epoch of reionization measurements with wide-field radio observations'. *The Astrophysical Journal*, 615, pp. 7.

Benson, Andrew J and Sugiyama, Naoshi and Nusser, Adi and Lacey, Cedric G, 2006. 'The epoch of reionization'. *Monthly Notices of the Royal Astronomical Society*, 369, PP. 1055–1080.

Penzias, Arno A and Wilson, Robert Woodrow., 1965. 'A measurement of excess antenna temperature at 4080 Mc/s.' *Astrophysical Journal*, 142, pp. 419–421.

Sofue, Yoshiaki, 2020. 'Rotation curve of the Milky Way and the dark matter density'. *Galaxies*, 8, pp.37.

Ramesh, R and Subramanian, KR and Sundararajan, MS and Sastry, Ch V, 1998. 'The gauribidanur radioheliograph' *Solar Physics*, 181, pp.439–453.

Hewish, A and Bell, SJ and Pilkington, JDH and Scott, PF and Collins, RA., (1969). 'Observation of a rapidly pulsating radio source (reprinted from Nature, February 24, 1968)'. *Nature*, 224, p.472.

Petroff, Emily and Hessels, JWT and Lorimer, DR., 2019. 'Fast radio bursts' *The Astronomy and Astrophysics Review*, 27, 4.

Cordes, James M and Shannon, Ryan M and Stinebring, Daniel R, 2016. 'Frequency-dependent dispersion measures and implications for pulsar timing' *The Astrophysical Journal*, 817, p.16.

Lyne, AG and Smith, F Graham, 1989. 'Pulsar rotation measures and the galactic magnetic field' *Monthly Notices of the Royal Astronomical Society*, 237, pp.533–541.

Singha, Jaikhomba and Surnis, Mayuresh P and Joshi, Bhal Chandra and Tarafdar, Pratik and Rana, Prerna and Susobhanan, Abhimanyu and Girgaonkar, Raghav and Kolhe, Neel and Agarwal, Nikita and Desai, Shantanu and others. (2021) 'Evidence for profile changes in PSR J1713+0747 using the uGMRT'. *Monthly Notices of the Royal Astronomical Society: Letters*, 507, pp. L57–L61.

Backer, DC and Hellings, RW., 1986. 'Pulsar timing and general relativity' *Annual review of astronomy and astrophysics.*, 24, pp. 537–575.

Tarafdar, Pratik and Nobleson, K and Rana, Prerna and Singha, Jaikhomba and Krishnakumar, MA and Joshi, Bhal Chandra and Paladi, Avinash Kumar and Kolhe, Neel and Batra, Neelam Dhanda and Agarwal, Nikita and others, 2022. 'The indian pulsar timing array: First data release'. *Publications of the Astronomical Society of Australia*, 39, e053.

Srivastava, Aman and Desai, Shantanu and Kolhe, Neel and Surnis, Mayuresh and Joshi, Bhal Chandra and Susobhanan, Abhimanyu and Chalumeau, Aurélien and Hisano, Shinnosuke and K, Nobleson and Arumugam, Swetha and others, 2023. 'Noise analysis of the Indian Pulsar Timing Array data release I'. *Physical Review D*, 108, p.023008.

Bhat, NDR and Tremblay, SE and Kirsten, Franz and Meyers, BW and Sokolowski, Marcin and Van Straten, W and McSweeney, SJ and Ord, SM and Shannon, RM and Beardsley, A and others. (2018) 'Observations of low-frequency radio emission from millisecond pulsars and multipath propagation in the interstellar medium'. *The Astrophysical Journal Supplement Series*, 238, p.1.

van Haarlem, Michael P and Wise, Michael W and Gunst, AW and Heald, George and McKean, John P and Hessels, Jason WT and de Bruyn, A Ger and Nijboer, Ronald and Swinbank, John and Fallows, Richard and others., (2013). 'LOFAR: The low-frequency array'. *Astronomy & astrophysics*, 556, pp. A2.

Ellingson, Steven W and Clarke, Tracy E and Cohen, Aaron and Craig, Joseph and Kassim, Namir E and Pihlstrom, Ylva and Rickard, Lee J and Taylor, Gregory B., 2009. 'The long wavelength array'. *Proceedings of the IEEE*, 97, pp. 1421–1430.

Tingay, Steven John and Goeke, Robert and Bowman, Judd D and Emrich, David and Ord, Stephen M and Mitchell, Daniel A and Morales, Miguel F and Booler, Tom and Crosse, Brian and Wayth, Randall B and others., 2013. 'The Murchison widefield array: the square kilometre array precursor at low radio frequencies'. *Publications of the Astronomical Society of Australia*, 30, pp.e007.

Amiri, M and Bandura, K and Berger, P and Bhardwaj, M and Boyce, MM and Boyle, PJ and Brar, C and Burhanpurkar, M and Chawla, P and Chowdhury, J and others., (2018). 'The CHIME fast radio burst project: system overview'. *The Astrophysical Journal*, 863, p.48.

DeBoer, David R and Parsons, Aaron R and Aguirre, James E and Alexander, Paul and Ali, Zaki S and Beardsley, Adam P and Bernardi, Gianni and Bowman, Judd D and Bradley, Richard F and Carilli, Chris L and others., 2017. 'Hydrogen epoch of reionization array (HERA)' *Publications of the Astronomical Society of the Pacific*, 129, pp.045001.

Dewdney, Peter E and Hall, Peter J and Schilizzi, Richard T and Lazio, T Joseph LW., 2016. 'The square kilometre array' *Proceedings of the IEEE*, 97, pp. 1482–1496.

Sastry, Ch V, 1989. 'The Gauribidanur radio observatory' *National Institute of Science Communication and Information Resources*.

Deshpande, A. A., and V. Radhakrishnan., 1992. 'Pulsar observations at 34.5 MHz using the Gauribidanur Telescope: I.' *Journal of astrophysics and astronomy*, 13.2, pp. 151–165.

Maan, Y., 2015. 'Discovery of low DM fast radio transients: Geminga pulsar caught in the act.' *The Astrophysical Journal*, 815(2), p.126 .

Bane, Kshiti J., Indrajit V. Barve, G. V. S. Gireesh, C. Kathiravan, and R. Ramesh., 2022. 'Prototype for pulsar observations at low radio frequencies using log-periodic dipole antennas.' *Journal of Astronomical Telescopes, Instruments, and Systems*, 8, 1 .

Isbell, D, 2003. 'Log periodic dipole arrays' *IRE transactions on antennas and propagation*, 8, p.260–267 .

Arul Pandian, B., Raghavendra Rao, K. B., Vinutha, C., Abhishek, R., Prabu, T., and Bagchi, J., 2022. 'A Novel LPDA Array for 130–350 MHz Pulsar observation at Gauribidanur-Initial Results.' In *43rd meeting of the Astronomical Society of India*, p. 49.

Foster, Griffin and Karastergiou, Aris and Paulin, Remi and Carozzi, TD and Johnston, Simon and van Straten, Willem, 2015. 'Intrinsic instrumental polarization and high-precision pulsar timing' *Oxford University Press*, 453, p.1489–1502 .

Arul Pandian B (2025) 'Arul16psp05/supplementary_materials: Gauribidanur Diamond Array'. *Zenodo*, doi: 10.5281/zenodo.15709357, <https://doi.org/10.5281/zenodo.15709357>.

Kraus, J.D. and Fleisch, D.A., 1999, 'Electromagnetics: With Applications'. *WCB/McGraw-Hill*, isbn: 9780071164290.

Kraus, John D and Moffet, Alan T. (1967), 'Radio Astronomy'. *American Journal of Physics*, 35, pp. 450–450.

Maan, Yogesh and Deshpande, Avinash A and Chandrashekhar, Vinutha and Chennamangalam, Jayanth and Rao, KB Raghavendra and Somashekhar, R and Anderson, Gary and Ezhilarasi, MS and Sujatha, S and Kasturi, S and others. (2013) 'RRI-GBT multi-band receiver: motivation, design, and development'. *The Astrophysical Journal Supplement Series*, 204, pp. 12.

Shankar, N Udaya and Dwarakanath, KS and Amiri, Shahram and Somashekhar, R and Girish, BS and Laus, Wences and Nayak, Arvind, 2009. 'A 50 MHz system for GMRT'. *arxiv.org*, [arXivpreprintarXiv:0905.1461](https://arxiv.org/abs/0905.1461).

de Lera Acedo, E and Razavi-Ghods, N and Troop, N and Drought, N and Faulkner, AJ, 2015. 'SKALA, a log-periodic array antenna for the SKA-low instrument: design, simulations, tests and system considerations'. *Experimental Astronomy*, 39, pp. 567–594.

Fiorelli, B and Acedo, E De Lera. (2014) 'On the simulation and validation of the Intrinsic Cross-Polarization Ratio for antenna arrays devoted to low frequency radio astronomy'. *IEEE*, pp. 2361–2364.

Kawano, Toru and Nakano, Hisamatsu, 2016. 'A grid array antenna composed of diamond-shaped cells' *IEEE*, pp.1–3.

Kawano, Toru and Nakano, Hisamatsu, 2017. 'A diamond-shaped grid array antenna printed on a dielectric substrate'. *IEEE* pp.105–107.

Hotan, AW and Bunton, JD and Chippendale, AP and Whiting, M and Tuthill, John and Moss, Vanessa A and McConnell, D and Amy, SW and Huynh, MT and Allison, JR and others, 2021, 'Australian square kilometre array pathfinder: I. system description'. *Cambridge University Press*, 38, p. e009.

Likhit, Anumanchi Agastya Sai Ram and Naveen, Katta and Pandian, B Arul and Abhishek, R and Prabu, Thiagaraj. (2025), 'Innovative Web Tool for Remote Data Acquisition and Analysis: Customized for SKA Low frequency Beamforming Test Bed LPDA Array at Gauribidanur Radio Observatory'. *Journal of Astrophysics and Astronomy*, 46.

Corey Satten. (2008) 'Lossless Gigabit Remote Packet Capture With Linux'. <https://staff.washington.edu/corey/gulp/>.

Corona, Paolo and Ferrara, Giuseppe and Gennarelli, Claudio. (1989) 'Measurement distance requirements for both symmetrical and antisymmetrical aperture antennas'. *IEEE*, pp. 990–995.

Yamaguchi, Ryo and Kimura, Yasuko and Komiya, Kazuhiro and Cho, Keizo, 2009. 'A far-field measurement method for large size antenna by using synthetic aperture antenna' *IEEE*, pp. 1730–1733.

Line, JLB and McKinley, B and Rasti, J and Bhardwaj, M and Wayth, RB and Webster, RL and Ung, D and Emrich, David and Horsley, L and Beardsley, A and others, 2009. 'In situ measurement of MWA primary beam variation using ORBCOMM' *Publications of the Astronomical Society of Australia*, 35, pp. e045.

Neben, AR and Bradley, RF and Hewitt, Jacqueline N and Bernardi, GIANNI and Bowman, JD and Briggs, Franklin and Cappallo, RJ and Deshpande, AA and Goeke, R and Greenhill, LJ and others, 2015. 'Measuring phased-array antenna beampatterns with high dynamic range for the Murchison Widefield Array using 137 MHz ORBCOMM satellites'. *AGU*, 50, pp.614–629.

Law, DC and Khorrami, JR and Sessions, WB and Shanahan, MK, 1997, 'Radiation patterns of a large UHF phased-array antenna: A comparison of measurements using satellite repeaters and patterns derived from measurements of antenna current distributions'. *IEEE Antennas and Propagation Magazine*, 39, pp. 88–93.

Harris, Charles R and Millman, K Jarrod and Van Der Walt, Stéfan J and Gommers, Ralf and Virtanen, Pauli and Cournapeau, David and Wieser, Eric and Taylor, Julian and Berg, Sebastian and Smith, Nathaniel J and others. (2020), 'Array programming with NumPy'. *Nature*, 585, pp. 357–362.

Perley, Richard A and Butler, Bryan J, 2017. 'An accurate flux density scale from 50 MHz to 50 GHz' *The Astrophysical Journal Supplement Series*, 230, pp. 7.

Remazeilles, M and Dickinson, C and Banday, AJ and Bigot-Sazy, M-A and Ghosh, T, 2015. 'An improved source-subtracted and destriped 408-MHz all-sky map'. *Monthly Notices of the Royal Astronomical Society*, 451, pp.4311–4327.

Robitaille, Thomas P and Tollerud, Erik J and Greenfield, Perry and Droettboom, Michael and Bray, Erik and Aldcroft, Tom and Davis, Matt and Ginsburg, Adam and Price-Whelan, Adrian M and Kerzendorf, Wolfgang E and others, 2013, 'Astropy: A community Python package for astronomy'. *Astronomy & Astrophysics*, 558, pp. A33.

Upadhyay, Kushagra and Joshi, Bhuwan and Mitra, Prabir K and Bhattacharyya, Ramit and Oberoi, Divya and Monstein, Christian. (2019), 'Solar radio observation using CALLISTO at the USO/PRL, Udaipur'. *IEEE*, pp. 1–6.

Arul Pandian B, Joydeep Bagchi, Prabu T, K.B.Raghavendra Rao, Vinutha Chandrashekhar, & Hobbs, M. (2025). GBD-DART - II: Gauribidanur Diamond Array Radio Telescope: Pulsar Signal Processing Pipeline, with Initial Results Observing Five Bright Pulsars (In Preparation,2026).

Hunter, J. D., 2007. 'Matplotlib: A 2D graphics environment' *Computing in Science & Engineering*, 9, pp. 90–95.

van Straten, W., & Bailes, M. (2011). DSPSR: digital signal processing software for pulsar astronomy. *Publications of the Astronomical Society of Australia*, 28(1), 1–14.

Hotan, A. W., van Straten, W., & Manchester, R. N. (2004). PSRCHIVE and PSRFITS: an open approach to radio pulsar data storage and analysis. *Publications of the Astronomical Society of Australia*, 21(3), 302–309.

Lorimer, Duncan Ross and Kramer, Michael, 2015. 'Handbook of pulsar astronomy'. *Cambridge university press*, 4, pp.4311–4327.

Girish, BS and Reddy, S Harshavardhan and Sethi, Shiv and Srivani, KS and Abhishek, R and Ajithkumar, B and Bhatramakki, Sahana and Buch, Kaushal and Chaudhuri, Sandeep and Gupta, Yashwant and others, 2023, 'Progression of digital-receiver architecture: From MWA to SKA1-Low, and beyond'. *Journal of Astrophysics and Astronomy*, 44, pp. 28.

Fitria, Tira Nur. (2021), 'Grammarly as AI-powered English writing assistant: Students' alternative for writing English'. *Metathesis: Journal of English Language, Literature, and Teaching*, 5, pp. 65–78.

Fitria, Tira Nur. (2021), 'QuillBot as an online tool: Students' alternative in paraphrasing and rewriting of English writing'. *Englisia: Journal of Language, Education, and Humanities*, 9, pp. 183–196.

Adithya Poder, 2025. "RRI Astronomy Summer School (RASS) - 2025", <https://github.com/pi-r2-dev/RASS-2025.git>

Mahek Patel, 2025. "RRI Astronomy Summer School (RASS) - 2025",, <https://github.com/Mahek566/RASS-Summer-School-Pulsar-Project.git>